Annales
Geophysicae

Open Access

EGU

Atmospheric CO₂ source and sink patterns over the Indian region

Suvarna Fadnavis[1]**, K. Ravi Kumar**[2,4]**, Yogesh K. Tiwari**[1]**, and Luca Pozzoli**[3]

[1]Centre for Climate Change Research, Indian Institute of Tropical Meteorology, Pune, India
[2]Department of Environmental and Geochemical Cycle Research, JAMSTEC, Yokohama, Japan
[3]Eurasia Institute of Earth Sciences, Istanbul Technical University, Istanbul, Turkey
[4]National Institute of Polar Research, Tokyo, Japan

Correspondence to: Yogesh K. Tiwari (yktiwari@tropmet.res.in)

Abstract. In this paper we examine CO_2 emission hot spots and sink regions over India as identified from global model simulations during the period 2000–2009. CO_2 emission hot spots overlap with locations of densely clustered thermal power plants, coal mines and other industrial and urban centres; CO_2 sink regions coincide with the locations of dense forest. Fossil fuel CO_2 emissions are compared with two bottom-up inventories: the Regional Emission inventories in ASia (REAS v1.11; 2000–2009) and the Emission Database for Global Atmospheric Research (EDGAR v4.2) (2000–2009). Estimated fossil fuel emissions over the hot spot region are $\sim$ 500–950 $\mathrm{gC\,m^{-2}\,yr^{-1}}$ as obtained from the global model simulation, EDGAR v4.2 and REAS v1.11 emission inventory. Simulated total fluxes show increasing trends, from $1.39 \pm 1.01\,\%\,\mathrm{yr^{-1}}$ ($19.8 \pm 1.9\,\mathrm{TgC\,yr^{-1}}$) to $6.7 \pm 0.54\,\%\,\mathrm{yr^{-1}}$ ($97 \pm 12\,\mathrm{TgC\,yr^{-1}}$) over the hot spot regions and decreasing trends of $-0.95 \pm 1.51\,\%\,\mathrm{yr^{-1}}$ ($-1 \pm 2\,\mathrm{TgC\,yr^{-1}}$) to $-5.7 \pm 2.89\,\%\,\mathrm{yr^{-1}}$ ($-2.3 \pm 2\,\mathrm{TgC\,yr^{-1}}$) over the sink regions. Model-simulated terrestrial ecosystem fluxes show decreasing trends (increasing CO_2 uptake) over the sink regions. Decreasing trends in terrestrial ecosystem fluxes imply that forest cover is increasing, which is consistent with India State of Forest Report (2009). Fossil fuel emissions show statistically significant increasing trends in all the data sets considered in this study. Estimated trend in simulated total fluxes over the Indian region is $\sim 4.72 \pm 2.25\,\%\,\mathrm{yr^{-1}}$ ($25.6\,\mathrm{TgC\,yr^{-1}}$) which is slightly higher than global growth rate $\sim 3.1\,\%\,\mathrm{yr^{-1}}$ during 2000–2010.

Keywords. Atmospheric composition and structure (pollution – urban and regional)

1 Introduction

Atmospheric carbon dioxide (CO_2) is regarded as one of the main greenhouse gases that cause global warming and force climate change. The present CO_2 increase is attributed to anthropogenic emissions which directly contribute to global warming (IPCC, 2007). Since the pre-industrial era atmospheric CO_2 concentrations have increased by $\sim 40\,\%$ (Hungershoefer et al., 2010) of which the major part is from fossil fuel combustion. The major source of CO_2 is fossil fuels combustion. The other sources are land use changes, the ocean and animal respiration, while it is removed by plants through photosynthesis, dissolution in the ocean and by carbon deposition (Peters et al., 2007). On the regional scale there is tremendous diversity in CO_2 sources and sinks due to varied anthropogenic activity and ecosystems. The industrialization of eastern Asia has influenced the chemical climate of India through transport processes. Also, rapid economic growth, industrialization, growing cities, increasing traffic and higher levels of energy consumption have led to higher emissions of greenhouse gases in India (INCCA, 2010). Pockets of heavy pollution are being created by emissions from major industrial zones and megacities where vehicle numbers are rapidly increasing (Garg et al., 2001). The high influx of population to urban areas, increase in consumption patterns and unplanned urban and industrial development contribute to increasing CO_2 emissions. Electricity generation is the largest producer of CO_2 emissions. Power plants, most notably coal-fired ones, are among the largest CO_2 emitters (DoE and EPA, 2000). Coal-based power plants in India account for about 53 % of installed capacity and contribute to more than 60 % of electricity generation (Behera et al., 2011). Coal is the mainstay of the Indian energy sector

and contributes almost 73 % of total CO_2 emissions (Garg et al., 2001). It can be expected that CO_2 emissions from coal-fired power plants will continue for many decades – probably with significantly increased emissions as the construction of coal-fired power plants is accelerating rapidly in India (Shindell and Faluvegi, 2010). Garg et al. (2001) reported that anthropogenic CO_2 emissions over India increased by 186 Tg during the period 1990–1995. They reported a direct correlation between coal consumption and CO_2 emissions over Indian districts. Between 1950 and 2008, India experienced a dramatic growth in fossil fuel CO_2 emissions, averaging 5.7 % a year, and became the world's third largest fossil fuel CO_2-emitting country (IEA, 2011).

As the distribution of atmospheric CO_2 reflects both spatial and temporal evolutions as well as the magnitude of surface fluxes (Tans et al., 1990), it is essential to know its sources and sinks, their spatial distribution and variability in time. There are top-down and bottom-up approaches to estimate carbon sources and sinks. In a top-down approach land–air surface flux distributions are identified by inverse modelling of atmospheric transport using CO_2 concentration observations (Rayner et al., 1999; Bousquet et al., 2000; Gurney et al., 2002; Rödenbeck et al., 2003). The bottom-up approach combines local information on the location and activity of the sources and the corresponding emission factors, for each emission sector (e.g. road transport, industry, power generation, residential heating, etc.).

The knowledge of spatio-temporal variability of CO_2 surface fluxes is essential as transported CO_2 alters the atmospheric heating and thereby the circulation patterns and hydrological cycle. Several model simulation studies have analysed the influence of increased CO_2 future scenarios on monsoon dynamics and precipitation (Cherchi et al., 2011; May 2011; Meehl and Washington, 1993; Meehl et al., 2000). Furthermore, other studies have shown that tropospheric CO_2 concentrations can be influenced by the strength of the monsoon and El Niño circulations (Mandal et al., 2006; Jiang et al., 2010; Schuck et al., 2010; Wang et al., 2011). Tiwari et al. (2011) and Bhattcharya et al. (2009) have shown effects of the Indian summer monsoon on the distribution of atmospheric CO_2. Latha and Murthy (2012) reported the variation of CO_2 during the pre-monsoon season.

Studies related to the variability of CO_2 fluxes over the Indian region are sparse. A regional assessment of greenhouse gases including CO_2 emissions from different sectors (e.g. electric power generation, industries, road, other transport etc.) in India during the period 1990–1995 has been conducted by Garg et al. (2001). They reported that CO_2 emissions from the largest emitters were increased by 8.1 % in 1995 with respect to 1990. Coal-based thermal plants were identified as major emitters. Later, Garg et al. (2006) estimated sectoral trends in greenhouse gases over India for the period 1985–2005. CO_2 removal by land-use and land-use change activities were not considered. Their emissions inventory showed that the power generation share in India's

CO_2 emissions increased from 33 to 52 % during the period 1985–2005 and that the majority of it comes from coal and lignite consumption.

As shown above, the spatio-temporal variation of CO_2 sources and sinks over the Indian region have not yet been addressed. Hence in this study we study CO_2 sources and sinks over the Indian region. CO_2 hot spot and sink regions are identified from Carbon Tracker (CT-2010) fluxes for the latest decade (2000–2009) over the Indian land mass (8–40° N, 60–100° E). Long-term trends are estimated over the hot spots and sink regions. Trends in fossil fuel emissions are compared with two bottom-up emission inventories: the Regional Emission inventory in ASia (REAS v1.11) for the period 2000–2009 and the Emission Database for Global Atmospheric Research (EDGAR v4.2) for the period 2000–2009. The paper is organized as follows: Sect. 2 gives details of the CT-2010 data, REAS v1.11, EDGAR v4.2 emission inventories and methods of analysis used in this study. Section 3 illustrates CO_2 emission hot spots and sinks as identified from CT-2010 fluxes. The regional distribution of possible sources and sinks is discussed. CT-2010 fossil fuel emissions are compared with REAS v1.11 and EDGAR v4.2 emission inventories. Trend estimates obtained from CT-2010, REASv1.11 and EDGAR v4.2 are also discussed. A summary of the results obtained in this study and final conclusions are given in Sect. 4.

2   Data and analysis

CT-2010 is a state-of-the-art data assimilation system that calculates net surface land and ocean CO_2 fluxes from a set of 28 000 high-precision CO_2 mole fraction observations in the global atmosphere (Peters et al., 2007). It forecasts atmospheric CO_2 mole fractions around the globe from a combination of CO_2 surface exchange models and an atmospheric transport model driven by meteorological fields from the European Centre for Medium-Range Weather Forecasts (ECMWF). The four surface flux modules used are: (1) prescribed anthropogenic fossil fuel emissions, (2) prescribed fire emissions (van der Werf et al., 2006), (3) first-guess (a priori) terrestrial net ecosystem exchange (NEE) (van der Werf et al., 2006) and (4) a priori net ocean surface fluxes (Jacobson et al., 2007). This results in a 4-D atmospheric CO_2 distribution which is then interpolated for the times and locations where atmospheric observations exist. Using an ensemble Kalman filter optimization scheme with a 5-week lag, the initial land and ocean net surface fluxes are adjusted up or down using a set of weekly and regional flux scaling factors to minimize differences between the forecasted and observed CO_2 mole fractions (Peters et al., 2007). Since few atmospheric data are available over the Indian region, Carbon Tracker used prior fluxes. Carbon Tracker uses fossil fuel emission data from the Carbon Dioxide Information Analysis Center (CDIAC) and the Emission Database for Global

Atmospheric Research (EDGAR v4.2), data of fires from the Global Fire Emissions Database (GFED)/MODIS and biosphere uptake patterns from the Carnegie-Ames-Stanford-Approach (CASA)-GFED2.

The fossil fuel emission inventory used in Carbon Tracker is derived from independent global total and spatially resolved inventories. Data on annual global total fossil fuel CO_2 emissions are from the Carbon Dioxide Information and Analysis Center (CDIAC) (Boden et al., 2011), and extend through 2007. In order to extrapolate these fluxes to 2008 and 2009, relative increases for each fuel type (solid, liquid and gas) in each country from the BP Statistical Review of World Energy for 2008 and 2009 is estimated. The spatial distributions of CO_2 fluxes are obtained in two steps: First, the coarse scale flux distribution country totals from Boden et al. (2011) are mapped onto a $1° \times 1°$ grid. Then the country totals are distributed within the countries according to the spatial patterns from the EDGAR-v4.2 inventories (Olivier and Berdowski, 2001), which are annual estimates also at $1° \times 1°$ resolution. The biosphere model CASA calculates global carbon fluxes using input from weather models to drive biophysical processes, as well as the satellite-observed Normalized Difference Vegetation Index (NDVI) to track plant phenology. The CASA model output used was driven by year-specific weather and satellite observations, and including the effects of fires on photosynthesis and respiration (van der Werf et al., 2006; Giglio et al., 2006). This simulation gives $1° \times 1°$ global fluxes on a monthly time resolution. In this work, we use fluxes from CT-2010 at $1° \times 1°$ resolution for the period 2000–2009. CO_2 fluxes are taken from the Carbon Tracker web site (ftp://aftp.cmdl.noaa.gov/products/carbontracker/co2/CT2010/).

To analyse the reliability of CT-2010 data over the Indian region, we compare CT-2010 concentrations with surface measurements over the Indian station Cape Rama (15.08° N, 73.83° E) since CO_2 flux measurements are not available. CO_2 measurements over Cape Rama are taken from http://ds.data.jma.go.jp/gmd/wdcgg/.

Figure 1 shows the temporal variation of CT-2010 CO_2 concentrations at 1012 hPa (at the grid centred at 15.08° N, 73.83° E) and CO_2 measurements at surface over Cape Rama (15.08° N, 73.83° E) from 1 September 2000 to 15 October 2002 and 1 July 2009 to 26 December 2010. CO_2 measurements are not available during the period 16 October 2002 to 30 June 2009. CT-2010 CO_2 concentrations and measurements at Cape Rama are presented in Fig. 1 at intervals of 15 days. CT-2010 concentrations are plotted at the same time. Figure 1 shows the good agreement of Carbon Tracker measurements with observations, which gives us some confidence on the ability of CT-2010 to determine CO_2 fluxes, even if it does not use any observational CO_2 data over India.

The CT-2010 fossil fuel emissions are compared with emission obtained from bottom-up inventories: EDGAR v4.2 and the REAS v1.11. The EDGAR v4.2 emissions (ex-
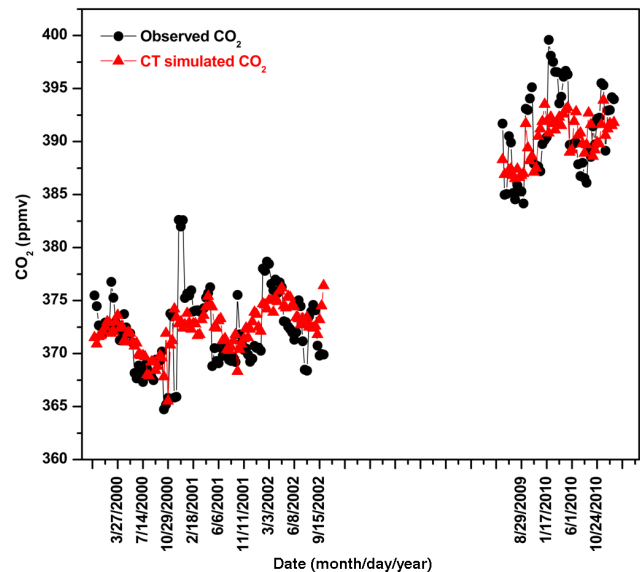

Figure 1. Temporal variation of CO_2 measurements during the periods 2000–2002 and 2009–2010 at surface over an Indian station (Cape Rama, 15.08° N, 73.83° E) indicated as -•- (in black) and Carbon Tracker CO_2 concentration at the grid centred at 15.08° N, 73.83° E at 1012 hPa indicated as -▲- (in red).

cluding short-cycle organic carbon from biomass burning) for the period 2000–2009 at the resolution 0.1×0.1 are obtained from http://edgar.jrc.ec.europa.eu/overview.php?v=_42 and the REAS v1.11 emissions (fossil and biofuel combustion and industrial sources) at the 0.5×0.5 resolution are obtained from (http://www.jamstec.go.jp/frsgc/research/d4/emission.htm).

REAS v1.11 historical emissions for the period 2000–2003 and predicted emissions for the period 2004–2009 are combined to obtain emissions for the study period. A detailed description of REAS v1.11 and EDGARv4.2 emission inventories is given by Ohara et al. (2007) and JRC/PBL (2012) respectively.

A regression analysis was applied to monthly mean fossil fuel emissions, net terrestrial ecosystem fluxes and total (fossil fuel emission + net terrestrial ecosystem + fire emissions) CO_2 fluxes as obtained from CT-2010 (2000–2009) to estimate trends. We use a regression model described in detail by Fadnavis et al. (2006) and Randel and Cobb (1994). The general expression for the regression model equation can be written as follows:

$$\theta(t,z) = \alpha(z) + \beta(z).\ \text{Trend}\ (t) + \text{resid}(t), \tag{1}$$

where $\alpha(z)$ and $\beta(z)$ are the time-dependent 12-month seasonal trend coefficients and resid(t) represents the residues. To fit seasonal variability, the coefficients α and β in Eq. (1) all have the form $\alpha = (A1 + A2 \cos \omega t + A3 \sin \omega t + A4 \cos 2\omega t + A5 \sin 2\omega t + A6 \cos 3\omega t + A7 \sin 3\omega t)$, with $\omega = 2n\,12\ \text{months}^{-1}$. There are
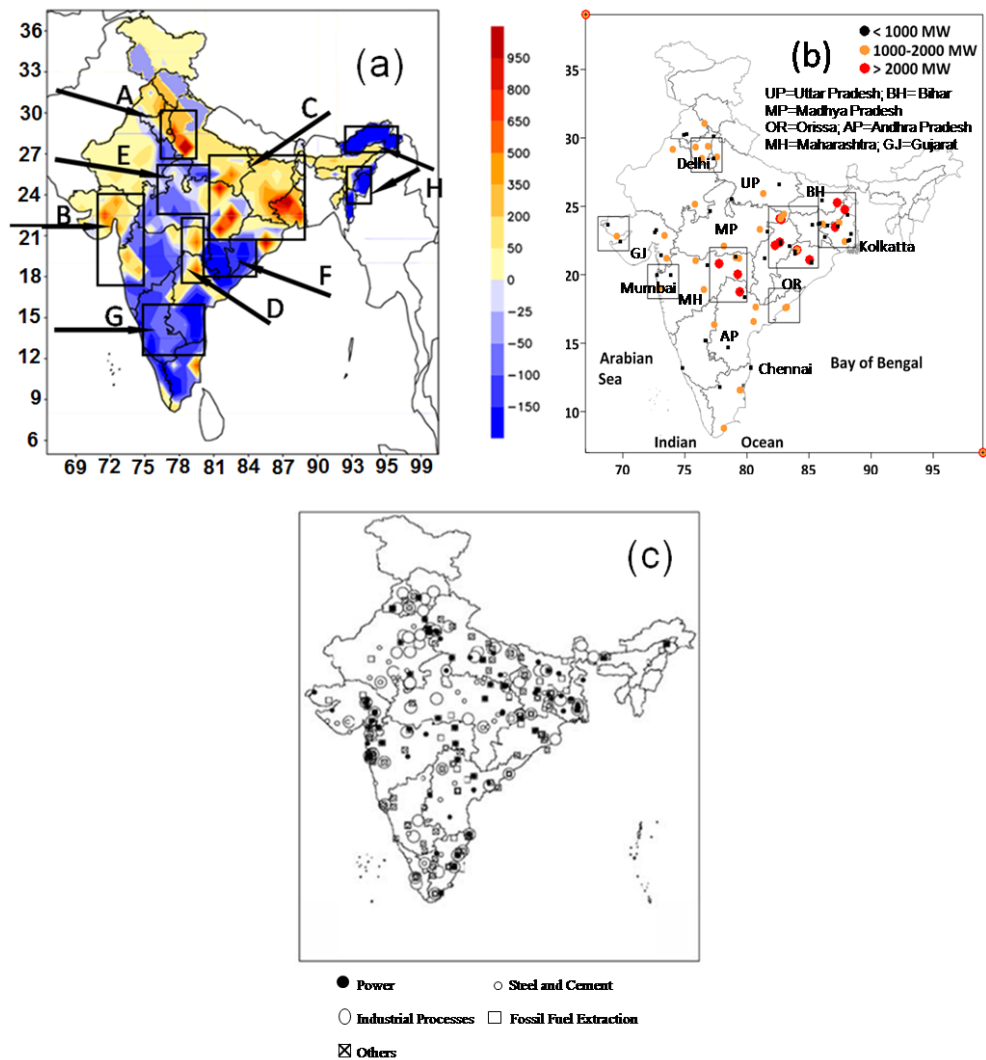
Figure 2. (a) Regional distribution of CO_2 total fluxes ($gC\,m^{-2}\,yr^{-1}$) as obtained from CT-2010 data averaged for the period 2000–2009 over the Indian land mass. **(b)** Regional distribution of major thermal power plants in India (adopted from Guttikunda and Jawear, 2014). **(c)** Regional distribution of large point sources over India (adopted from Garg et al., 2002).

seven parameters to be determined for each term in Eq. (1). It should be noted that the trend term in Eq. (1) is implicitly nonlinear. Further details of seasonally varying trend detection are given by Randel and Cobb (1994).

Trends are also estimated from yearly fossil fuel emission data obtained from REASv1.11 and EDGARv4.2 time series. Trends estimates from CT-2010 fossil fuel emissions are compared with trends obtained from EDGAR v4.2 (2000–2009) and REASv1.11 (2000–2009).

3   Results and discussions

3.1   Distribution of CO_2 fluxes over the Indian land mass

In order to identify CO_2 sources and sinks over the Indian continent (8–40° N, 68–100° E), CO_2 land atmosphere fluxes obtained from CT-2010 data are averaged for the period 2000–2009. CO_2 land atmosphere fluxes (total fluxes) are obtained from combined fossil fuel fluxes, terrestrial ecosystem fluxes and fire fluxes. Figure 2a shows the spatial distribution of total CO_2 fluxes over the Indian land mass. It can be seen that CO_2 fluxes vary between -150 and $950\,gC\,m^{-2}\,yr^{-1}$, and they are well spread over the Indian land mass. From atmospheric inversions (using regional and global transport models), Rivier et al. (2010) reported

CO$_2$ fluxes varying between -300 and $700\,\mathrm{g\,C\,m^{-2}\,yr^{-1}}$ over the European region. This indicates that CO$_2$ emissions are larger over the Indian region as compared to Europe. The regions emitting high CO$_2$ fluxes ($>500\,\mathrm{g\,C\,m^{-2}\,yr^{-1}}$) are considered as hot spots. CO$_2$ hot spots are observed over (1) the Delhi corridor region, (2) the Mumbai–Gujarat industrial corridor region, (3) North India (covering West Bengal–Jharkhand–Bihar) and (4) Central India (Maharashtra–Andhra Pradesh). For ease of reference, in the discussion that follows these regions are named as region A, region B, region C and region D respectively. Sinks (negative fluxes) are observed over (5) Madhya Pradesh, (6) Odisha–Chhattisgarh region, (7) Karnataka–Andhra Pradesh and (8) Northeast India (covering Arunachal Pradesh–Nagaland–Manipur–Mizoram). These sink regions are named as region E, region F, region G and region H respectively.

3.1.1 Distribution of CO$_2$ fluxes at hot spots

From Fig. 2a it is evident that CO$_2$ emissions are higher ($>200\,\mathrm{g\,C\,m^{-2}\,yr^{-1}}$) over the Indo-Gangetic Plain (which comprises region A and region C) as compared to other regions. CO$_2$ hot spots are densely clustered over region D. In order to understand the reason for observed high CO$_2$ emissions over the hot spot regions, we show the spatial distribution of CO$_2$ sources over the Indian land mass. Electricity and heat generation (coal-fired power plants, oil, gas) are the major CO$_2$ emitters (EPA, 2000). In India the majority of power plants are coal fired, and they are considered as large point sources (LPSs). Steel plants, cement plants, industrial processes (sugar, paper, etc), fossil fuel extraction are also LPSs of CO$_2$. Figure 2c (adapted from Garg et al. (2002) illustrates the distribution of these LPSs over India. It is interesting to compare Fig. 2a and c. High CO$_2$ fluxes are observed at these LPSs. In the Indo-Gangetic (IG) Plain thermal power plants, steel plants, refineries and other industries are densely concentrated. Furthermore, this region is densely populated, hence anthropogenic activities are also high: CO$_2$ emissions from transport, coal and wood burning for domestic cooking, ecosystem mass burning are common throughout the year (Garg et al., 2001). In addition to this, there are LPSs densely clustered near Delhi, along the eastern coal belt, and uniformly spread around the rest of the IG region (Garg et al., 2002; Dalvi et al., 2006; Ghude et al., 2008). Since power plants are the largest CO$_2$ emitters (DoE and EPA, 2000), it is interesting to observe the CO$_2$ hot spots and location of power plants simultaneously. Figure 2b shows the distribution of major thermal power plants in India. In region A (the Delhi corridor region) thermal power plants are located at Delhi, Faridabad, Panipat, Gautam Budh Nagar, Dadri and Harduaganj, where observed CO$_2$ fluxes are high ($>600\,\mathrm{g\,C\,m^{-2}\,yr^{-1}}$). In region B (Gujarat–Maharashtra) thermal power plants are located at Gandhi Nagar, Kheda, Janor, Nani Napoli and Nashik, where high CO$_2$ fluxes are collocated. Densely clustered

refineries and other industrial processes in the Mumbai–Gujarat region may also contribute to observed high CO$_2$ fluxes in this region. CO$_2$ fluxes $\sim 600\,\mathrm{g\,C\,m^{-2}\,yr^{-1}}$ are observed near the western border of West Bengal. It is observed that in this region thermal power plants at Sidhi, Durgapur, Suri, Vindhyachal and Singrauli are densely clustered. In region C, CO$_2$ fluxes greater than $500\,\mathrm{g\,C\,m^{-2}\,yr^{-1}}$ are observed near the Uttar Pradesh–Madhya Pradesh border where thermal power plants at Sidhi, Vindhyachal and Singrauli are located. In region D, CO$_2$ hot spots are observed near the Maharashtra–Andhra Pradesh border, where thermal power plants at Chandrapur, Ramagundam Jyothi Nagar, Chelpur and Khaparkheda are located. High CO$_2$ fluxes $\sim 600\,\mathrm{g\,C\,m^{-2}\,yr^{-1}}$ are observed near Pondicherry in Tamil Nadu. In this region, Athipattu, Ennore and Neyveli thermal power plants are collocated. A CO$_2$ emission hot spot is seen at the southern tip of India. Figure 2b shows the thermal power plants Kayamkulam and Tuticorin in this region, while Fig. 2c shows the location of LPSs at the same location.

This indicates that CO$_2$ emissions from power plants form the major contribution in hot spot regions. Garg et al. (2001) also observed that electric power generation contributes almost half of India's CO$_2$ emissions and that the majority comes from coal and lignite consumption. The User Guide for the CO$_2$ baseline database for the Indian power sector (2011) shows that total CO$_2$ emissions from the power sector increased to 548.3 Tg during the period 2008–2009 from 494.7 Tg in 2005–2006. Large numbers of coal mines are located in region C and region D. CO$_2$ emissions from frequent fire events at these mines will also contribute to these hot spots. Emissions from fire events at these refineries might have led to CO$_2$ fluxes of $500\text{--}1000\,\mathrm{g\,C\,m^{-2}\,yr^{-1}}$.

CO$_2$ emissions hot spots in regions A–D are collocated with thermal power plants, urban centres and industrial sources. The transport activities are most concentrated around the large urban and industrial centres. These regions are densely populated and hence a large amount of anthropogenic and vehicular emissions add to emissions from thermal and industrial sources. The transport sector sources contribute around 9.5 % to India's CO$_2$ equivalent greenhouse gas emissions (Garg et al., 2001). In India the number of vehicles is growing by about 5 % a year, with two-wheeled vehicles comprising 76 % to the total vehicular population (Ghude et al., 2008). Vehicle population in India is directly related to urban population (Dalvi et al., 2006).

3.1.2 Distribution of CO$_2$ fluxes in sink regions

In order to understand the reasons for the observed sink over regions E–G, we compared the spatial distribution of CO$_2$ fluxes with vegetation cover over India, as CO$_2$ is removed by plants through photosynthesis. Figure 3 shows forest cover over India during 2007 (adopted from https://en.wikipedia.org/wiki/Forestry_in_India). Comparison of
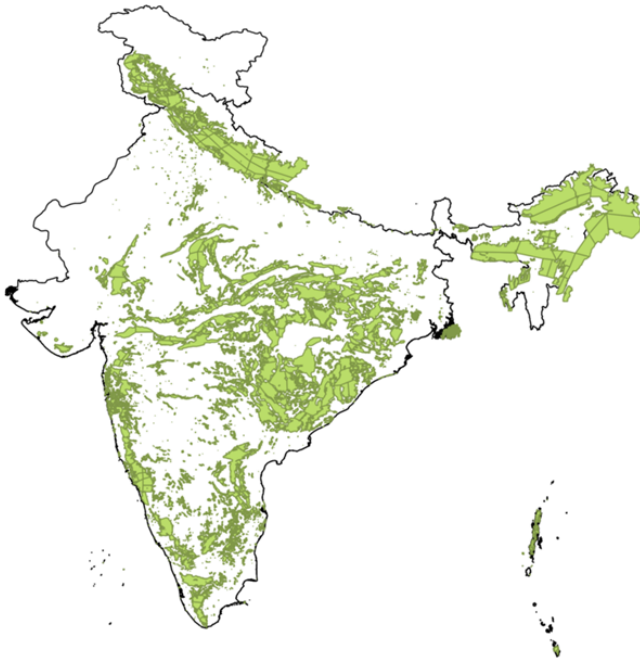
Figure 3. Forest cover map of India, February 2015 (from https://en.wikipedia.org/wiki/Forestry_in_India).

Figs. 2a and 3 shows that the regions with CO_2 sink (negative fluxes) are co-located with dense forest regions. For example region E (Madhya Pradesh), region F (Odisha–Chhattisgarh) and region H (Arunachal Pradesh, Manipur, Mizoram) are covered with dense forest and in such areas power plants and other industries are few. Region G is not covered with dense forest – the observed CO_2 sink may be due to moderate vegetation cover with open forest and due to the presence of a few power plants and industrial centres. Dense forest cover along the west coast of India (the Western Ghats) coincides with observed negative CO_2 fluxes (sink) ($\sim -100\,\mathrm{gC\,m^{-2}\,yr^{-1}}$). A CO_2 sink is observed over Shivalik mountain range at Uttarakhand and Himachal Pradesh as these mountain areas are covered with dense forest.

3.1.3   Distribution of CO_2 fossil fuel fluxes

Figure 4a shows the distribution of CO_2 emissions from anthropogenic fossil fuel burning averaged over the period 2000–2009. The simultaneous observations of Figs. 2a and 4a show that locations of emission of high amounts of CO_2 fossil fuel fluxes coincide with hot spots regions. The difference between CO_2 total fluxes and anthropogenic fossil fuel fluxes is shown in Fig. 4b. It indicates that fossil fuel fluxes dominate the total fluxes and largely contributes to the hot spots. Negative fluxes (indicative of terrestrial ecosystem fluxes) are observed at sink regions in Fig. 4b. CO_2 emissions $>20\,\mathrm{gC\,m^{-2}\,yr^{-1}}$ are observed in patches. This may be due to CO_2 emissions from fires.

Figure 4c and d show averaged CO_2 anthropogenic fossil fuel emissions obtained from EDGAR v4.2 for the period 2000–2009 and REAS v1.11 for the period 2000–2009 respectively. All the three data sets show CO_2 high emissions (500–$1000\,\mathrm{gC\,m^{-2}\,yr^{-1}}$) in the hot spot regions – CT-2010, EDGAR and REAS data sets show CO_2 emissions varying between 0 and $1000\,\mathrm{gC\,m^{-2}\,yr^{-1}}$. CO_2 hot spots are quite obvious in all the three data sets. From the REAS inventory Wang et al. (2012) reported that anthropogenic CO_2 emissions over China varied between 0.04 and 6.3×10^7 tons $\mathrm{yr^{-1}}$ during 2003–2005, whereas REAS v1.11 emissions vary between 0.2×10^6 and 4×10^6 ton $\mathrm{yr^{-1}}$ over the Indian land mass. This indicates that CO_2 emissions over China are higher than over India. Since the spatial resolution of EDGAR v4.2 data (0.1×0.1) is higher than REAS v1.11 (0.5×0.5) and CT-2010 (1×1), hot spots are more prominent in the EDGAR v4.2 data. High CO_2 fluxes ($>500\,\mathrm{gC\,m^{-2}\,yr^{-1}}$) near the location of LPSs (thermal power plants) are prominent in the EDGAR emissions inventory.

3.1.4   Distribution of CO_2 terrestrial ecosystem fluxes

Figure 5a shows the spatial distribution of CO_2 fluxes from terrestrial net ecosystem exchange (referred to as terrestrial ecosystem fluxes hereafter) averaged for the period 2000–2009. Positive fluxes represent emissions of CO_2 to the atmosphere, and negative fluxes indicate times when the land biosphere is a sink of CO_2. Figure 5a shows strong negative fluxes over the sink regions (regions E–H in Fig. 2a), along the west coast of India and in Punjab–Uttarakhand on the Shivalik mountain range where forest cover is dense (Fig. 3). CO_2 sinks are also observed in parts of other regions (for example regions B, C and D). This may be due to moderate forest cover in these regions. Figure 5b shows the change in forest cover (%) in India during 2005–2007 (India State of Forest Report, 2009). Although it does not show the change in forest cover during the study period, it indicates change in that region. It shows that most of the sink regions have gained forest cover of up to 0.5 %.

CO_2 fire fluxes (Fig. 6a) do not show much spatial variation. Patches of high CO_2 fluxes are observed over Northeast India (Assam, Nagaland Manipur, Arunachal Pradesh, Mizoram), along the west coast of India and over Chhattisgarh and Andhra Pradesh. Over India CO_2 fire fluxes vary from 4 to $45\,\mathrm{gC\,m^{-2}\,yr^{-1}}$. The observed high CO_2 fluxes from fire emissions may be due to forest fire events and fire events at coal mines and oil refineries (the majority of coal mines are clustered in regions C and D where forest cover is also dense), as patches of high CO_2 fluxes overlap with locations of dense forest coal mines and oil refineries. High CO_2 fluxes over West Bengal–Bihar, Chhattisgarh and Andhra Pradesh regions coincide with the coal mine locations. Figure 6b shows the distribution of oil refineries in India. High CO_2 fluxes are observed (Fig. 6a) near the location of oil refiner-
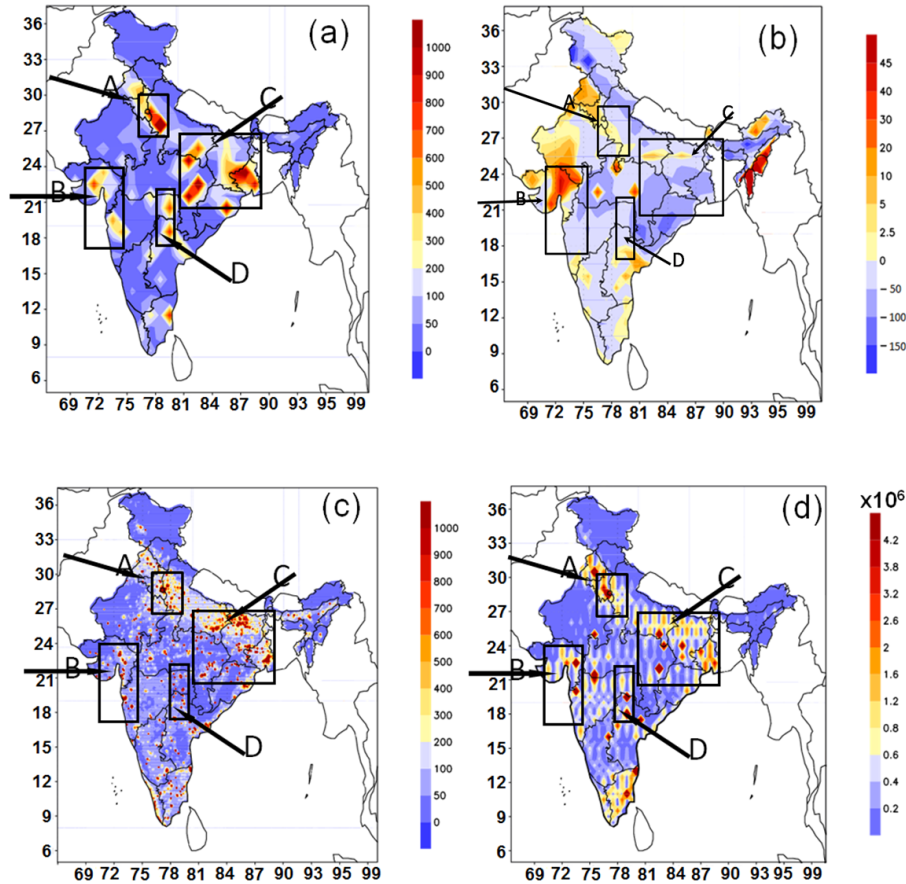
Figure 4. Regional distributions of **(a)** CT-2010 CO$_2$ fossil fuel fluxes (gC m^{-2} yr^{-1}) (2000–2009) and **(b)** difference between total and fossil fuel fluxes (gC m^{-2} yr^{-1}) as obtained from CT-2010 data averaged for the period 2000–2009 over the Indian land mass. **(c)** Regional distributions of EDGAR v4.2 CO$_2$ fossil fuel emission (gC m^{-2} yr^{-1}) (2000–2009) and **(d)** regional distributions of REASv1.11 CO$_2$ fossil fuel emissions (gC m^{-2} yr^{-1}) (2000–2009).
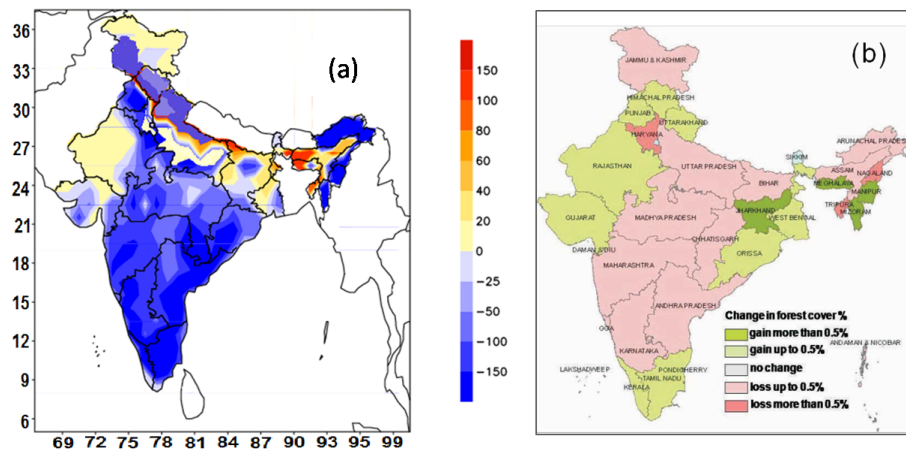

Figure 5. (a) Regional distributions of terrestrial ecosystem CO$_2$ fluxes (gC m^{-2} yr^{-1}) as obtained from CT-2010 data averaged for the period 2000–2009 over the Indian land mass. **(b)** Gain and loss of forest cover (%) in Indian states and union territories during 2005–2007 (India State of Forest Report, 2009).
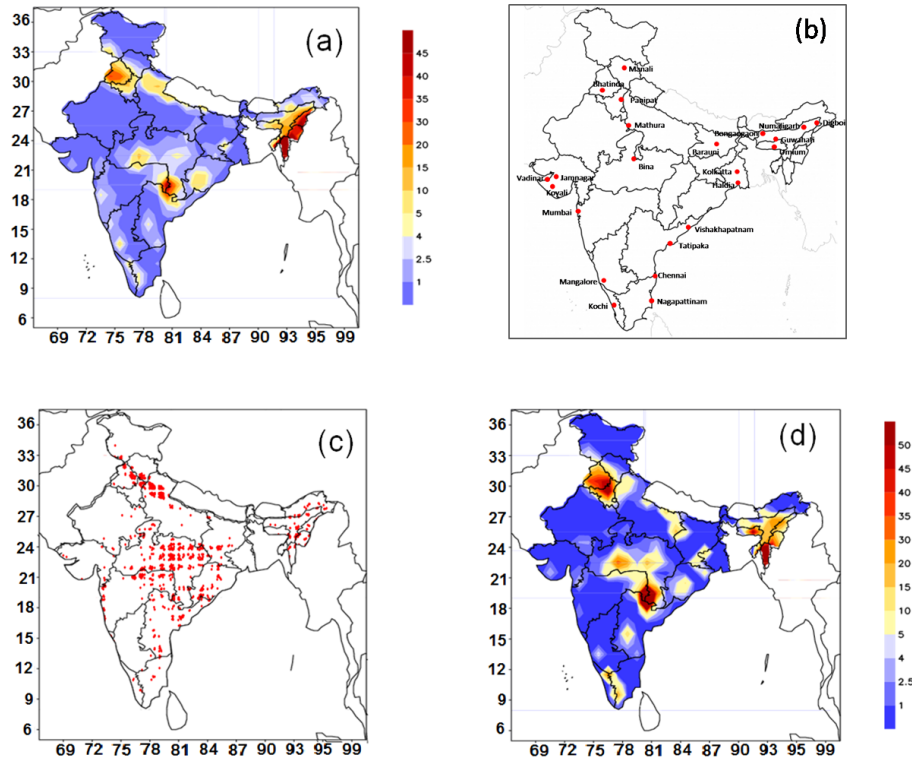
Figure 6. (a) Regional distributions of CO$_2$ fire fluxes (gC m^{-2} yr^{-1}) as obtained from CT-2010 data averaged for the period 2000–2009 over the Indian land mass. **(b)** Regional distribution of oil refineries in India. **(c)** Regional distribution of forest fire spots integrated for the year 2009 (Forest survey of India). **(d)** Regional distribution of CO$_2$ fire fluxes (gC m^{-2} yr^{-1}) as obtained from CT-2010 data averaged for the year 2009 over the Indian land mass.

ies in Northeast India, and along the west coast of India. High CO$_2$ fluxes ~ 15–30 gC m^{-2} yr^{-1} are observed near Digbol in Assam and Mangalore in Karnataka. Fire events at oil refineries might have contributed to observed the high CO$_2$ fluxes. CO$_2$ fluxes of ~ 4 gC m^{-2} yr^{-1} are observed near the west coast of India (Western Ghats) and fluxes of ~ 10–35 gC m^{-2} yr^{-1} are observed in Odisha, Chhattisgarh, Andhra Pradesh and Maharashtra regions and in the Shivalik mountain range. This may be related to forest fire events and fire events in coal mines occurring in these regions. In order to compare CO$_2$ fire fluxes with the distribution of fire spots, data obtained from the forest survey of India are analysed. When fire spot data integrated for the period 2000–2009 are plotted, a regional distribution of fire events was not evident due to the large amount of fire events during this period (figure not included). Hence the fire spot data integrated for the year 2009 are plotted in Fig. 6c. The simultaneous regional distribution of CO$_2$ fire fluxes (2–45 gC m^{-2} yr^{-1}) as obtained from CT-2010 averaged for the year 2009 is shown in Fig. 6d. CO$_2$ high (15–50 gC m^{-2} yr^{-1}) fluxes are observed in the regions of active fire events.

3.2 Trends in CO$_2$ fluxes over the Indian land mass

In order to determine trends in CO$_2$ fluxes over regions A–H, monthly mean CO$_2$ fluxes are averaged over the corresponding region to obtain the time series. These CT-2010 time series are then subjected to a regression model. Monthly mean trend coefficients obtained from the model are averaged to get the annual trend coefficient. Annual trend coefficients are calculated separately for fossil fuel, terrestrial ecosystem and total fluxes. Since fire events are occasional they are not subjected to regression analysis. Estimated trends over regions A–H are given in Table 1.

3.2.1 Trends in CO$_2$ total fluxes

CO$_2$ total fluxes (combined Fossil, Ecosystem, and Fire) show statistically significant increasing trends (at 95 % confidence level) over hot spot regions (regions A–D) and negative (decreasing) trends over the sink regions (E–H). Trends over the regions G and H are not statistically significant. The negative (decreasing) trends over CO$_2$ sink regions can be explained from terrestrial ecosystem fluxes (discussed later). Over the Indian hot spot regions trends vary between 1.39 ± 1.01 % yr^{-1} (19.8 ± 1.9 TgC yr^{-1}) and 6.7 ± 0.54 % yr^{-1} (97 ± 12 TgC yr^{-1}). A strongly increas-

Table 1. Annual trend in % yr^{-1} (TgC yr^{-1}) in CT-2010 CO$_2$ fluxes (total/fossil fuel/terrestrial ecosystem fluxes) over regions A–H. Annual trends estimated in fossil fuel emissions as obtained from REAS v1.11 (for the period 2000–2009) and EDGAR v4.2 (for the period 2000–2009) over regions A–H. Regions A–H refer to the CO$_2$ emission hot spots and sink regions as marked in Fig. 2a.

Sr. No.	Region	Trend in % yr^{-1} (TgC yr^{-1}) in total fluxes	Trend in % yr^{-1} (TgC yr^{-1}) in fossil fuel emissions CT-2010	Trend in % yr^{-1} (TgC yr^{-1}) in fossil fuel emissions REASv1.11 (2000–2009)	Trend in % yr^{-1} (TgC yr^{-1}) in fossil fuel emissions EDGARv4.2 (2000–2009)	Trend in % yr^{-1} (TgC yr^{-1}) in terrestrial ecosystem fluxes. CT-2010
1	Region A (Delhi corridor region)	3.25 ± 1.8 (30 ± 1.7)	4.37 ± 0.28 (23 ± 1.5)	3.36 ± 0.13 (20 ± 5.8)	3.81 ± 0.52 (22 ± 1.5)	1.56 ± 1.1 (4 ± 2)
2	Region B (Mumbai–Gujarat)	6.21 ± 2.77 (34 ± 5.7)	4.7 ± 0.26 (30 ± 2)	3.7 ± 0.16 (25 ± 6.6)	3.93 ± 0.53 (27.9 ± 1.95)	1.68 ± 1.23 (4 ± 0.5)
3	Region C (North India)	6.7 ± 0.54 (97 ± 12)	4.84 ± 0.34 (80 ± 4.8)	3.32 ± 0.1 (76 ± 21.1)	4.57 ± 0.48 (79.3 ± 4.2)	−3.75 ± 1.89 (−1.9 ± 0.11
4	Region D (Central India)	1.39 ± 1.01 (19.8 ± 1.9)	4.8 ± 0.3 (18 ± 1.1)	3.8 ± 0.14 (13.5 ± 7.2)	4.33 ± 0.5 (15.5 ± 1.0)	−2.5 ± 1.8 (−4 ± 1)
5	Region E (Madhya Pradesh)	−3.2 ± 2.48 (−2 ± 0.1)	5.4 ± 0.47 (1 ± 0.1)	3.19 ± 0.17 (0.8 ± 0.69)	3.9 ± 0.418 (1 ± 1)	−3.97 ± 2.0 (−1.7 ± 0.6)
6	Region F (Odisha-Chhattisgarh region)	−5.7 ± 2.89 (−2.3 ± 2)	5.5 ± 0.51 (7.2 ± 1)	3.31 ± 0.19 (6.13 ± 3.21)	4.4 ± 0.39 (6.4 ± 0.5)	−3.68 ± 3.2 (−2 ± 1.2)
7	Region G (Karnataka-Andhra Pradesh)	−1.85 ± 2.3 (−1.9 ± 3)	5.0 ± 0.35 (7.0 ± 0.64)	3.73 ± 0.15 (6.01 ± 2.32)	3.3 ± 0.4 (6.2 ± 1.0)	−2.27 ± 3.0 (−2.2 ± 2.3)
8	Region H (Northeast India)	−0.95 ± 1.51 (−1 ± 2)	5.2 ± 0.2 (4.7 ± 0.1)	3.92 ± 0.18 (4.2 ± 2.6)	3.0 ± 0.42 (4.4 ± 2.2)	−3.09 ± 5.0 (1.8 ± 1.8)

ing trend 6.7 ± 0.54 % yr^{-1} (97 ± 12 TgC yr^{-1}) is observed in region C. In this region LPSs are densely clustered as there are a number of power plants, steel plants, cement plants, industrial processes and fossil fuel extraction plants (see Fig. 2c). Moreover, this region overlaps with coal mines (fire events in coal mines contribute to the increase in the CO$_2$ amounts). Also this region is densely populated, hence anthropogenic CO$_2$ emission is high. In India the majority of power plants use coal as fuel. The power plants located in eastern regions have seen maximum annual growth of 2.2 % during the period 2003–2008 (Behera et al., 2011). Thus expansion of power plants clustered in this region during the last few years might have contributed to the strongly increasing observed trend. A similarly high CO$_2$ trend 6.21 ± 2.77 % yr^{-1} (34 ± 5.7 TgC yr^{-1}) is also observed over region B (Mumbai–Gujarat) where LPSs are densely clustered. Increasing CO$_2$ trends over region A (the Delhi corridor)

3.25 ± 1.8 % yr^{-1} (30 ± 1.7 TgC yr^{-1}) and region D (Central India) ∼ 1.39 ± 1.01 % yr^{-1} (19.8 ± 1.9 TgC yr^{-1}) are also observed. Observed trends over region A (Delhi corridor) are less than that of regions B and C. This may be due to reduced coal and oil consumption in Delhi during the last decade (Garg et al., 2001).

3.2.2 Trends in CO$_2$ fossil fuel fluxes

CT-2010 CO$_2$ fluxes from fossil fuel burning show statistically significant increasing trends over all the regions (A–H). Trend values vary between 4.37 ± 0.28 % yr^{-1} (23 ± 1.5 TgC yr^{-1}) (at region A) and 5.5 ± 0.51 % yr^{-1} (7.2 ± 1 TgC yr^{-1}) (at region F). CT-2010 did not optimize fossil fuel emission. Therefore, the trends calculated for fossil fuel emissions may reflect the bottom-up data used (e.g. EDGAR v4.2) as a priori fluxes. Trends are also estimated from yearly EDGAR v4.2 and REAS v1.11 emission inventories. All the three data sets show

Table 2. Yearly variation of CO_2 fluxes (gC m^{-2} yr^{-1}) from fossil fuel over region A (Delhi corridor), region B (Mumbai–Gujarat), region C (North India), region D (Central India), region E (Madhya Pradesh), region F (Odisha–Chhattisgarh), region G (Karnataka–Andhra Pradesh), region H (Northeast India).

	Region A	Region B	Region C	Region D	Region E	Region F	Region G	Region H
2000	244.70	107.40	233.70	113.0	27.76	24.22	38.32	17.40
2001	252.90	110.70	241.90	116.80	28.73	25.06	39.66	17.99
2002	259.00	113.60	248.00	119.60	29.40	25.63	40.58	18.40
2003	271.00	118.8	259.60	125.20	30.77	26.83	42.48	19.29
2004	283.90	124.60	272.00	131.10	32.22	28.10	44.48	20.20
2005	298.90	131.00	286.50	138.10	33.90	29.57	46.82	21.27
2006	318.60	139.60	305.20	147.20	36.31	31.66	50.10	22.76
2007	333.20	146.90	317.30	153.70	40.50	35.13	55.37	25.33
2008	358.80	158.20	341.50	165.50	43.61	37.83	59.62	27.26
2009	378.90	167.00	360.60	174.70	46.05	39.94	62.95	28.77

statistically significant increasing trends over all the regions. Trends estimated from REASv1.11 (3.19 ± 0.17 (0.8 ± 0.69 TgC yr^{-1}) and 3.92 ± 0.18 % yr^{-1} (4.2 ± 2.6)) and EDGAR v4.2 (3.0 ± 0.42 % yr^{-1} (4.4 ± 2.2 TgC yr^{-1}) and 4.57 ± 0.48 % yr^{-1} (79.3 ± 4.2 TgC yr^{-1})) emission inventories are less than CT-2010. The trends in CT-2010 fluxes are close to trend values in EDGAR v4.2, as CT-2010 used EDGAR v4.2 as a priori fluxes. The differences in trend values may be partially due to the difference in time period of the data sets (EDGAR v4.2 emission inventory is for the period 2000–2009 while the REAS v1.11 time series is obtained by combining historical (2000–2003) and prediction (2004–2009) emissions) and partially because of differences in species and emission sources: REAS v1.11 emissions are from fossil and bio-fuel combustion and industrial sources while EDGAR v4.2 emissions are from fossil fuel excluding short-cycle organic carbon from biomass burning. The Carbon Budget (2010) report shows that over India CO_2 emissions from fossil fuel increased ~ 9.4 % during the period 1990–2010. From the emission inventory of greenhouse gases, for 1990 and 1995, Garg et al. (2001) also observed growth of CO_2 emissions (~ 8.1 % annual growth) from fossil fuel over India. The IEA (2011) reported growth in fossil fuel CO_2 emissions of ~ 5.7 % during the period 1950–2008. Similar increasing trends are also observed in CT-2010. It should be noted that fossil fuel fluxes show increasing trends over the sink regions (E–H). Table 2 indicates the yearly variation of CO_2 emissions from fossil fuel over regions A–H. It can be seen that during all the years the amount of CO_2 emissions are less over the sink regions (E–H) as compared to over the hot spots regions (A–D). It should be noted that although the amount of CO_2 emissions are relatively less, emission rates are increasing over the period. This may be due to increasing anthropogenic activities such as industrialization, increasing population and urbanization.

3.2.3 Trends in terrestrial ecosystem CO_2 fluxes

CT-2010 terrestrial ecosystem fluxes show negative trends (decreasing) (more CO_2 uptake by increasing vegetation cover) over all the regions except regions A and B. Increasing trends in regions A and B indicate that the CO_2 sink is decreasing over the period. Figure 5b shows the spatial distribution of change in forest cover (%) during the period 2005–2007. It shows that this region lost more than 0.5 % of forest cover. Decreasing forest cover with time will decrease CO_2 uptake which might have resulted from the observed increasing terrestrial ecosystem fluxes. Statistically significant negative trends (decreasing) in terrestrial ecosystem fluxes over regions C, D and F may be due to increasing forest cover. Figure 5b shows that these regions (or parts of these regions) have gained forest by up to 0.5 % or more than 0.5 % during the period 2005–2007 (India State of Forest Report, 2009). Over the last two decades, progressive national forestry legislation and policies in India aimed at conservation and sustainable management of forests have reversed deforestation and have transformed India's forests into a significant net sink of CO_2 (India State of Forest Report, 2009). Forest cover over India in 1997 was 65.96 million hectares which increased to 69.09 million hectares by 2007. This indicates that India has gained forest cover of ~ 3.13 million hectares (4.75 %) during the period 1997–2007 (India State of Forest Report, 2009). It should be noted that over sink regions G and H, negative (decreasing) trends are not statistically significant. This may be due to deforestation in these areas. Figure 5b shows that these regions have lost forest by up to 0.5 % or more than 0.5 %.

The time series of total fluxes (fossil fuel, terrestrial ecosystem fluxes, fire) over regions A–H are averaged to obtain one time series representing the Indian region. Trends in total fluxes over the Indian region (covering source and sink regions) show increasing trends of $\sim 4.72 \pm 2.25$ % yr^{-1} (25.6 TgC yr^{-1}), indicating that CO_2 emissions from fossil fuel are more than the uptake by vegetation. The Carbon

Budget (2010) report shows that the global CO_2 emissions growth rate was $\sim 3.1\,\%\,\mathrm{yr}^{-1}$ during the period 2000–2010, which is slightly lower than the estimated growth rate over India.

Thus our analysis indicates that effort towards conservation and the reversal of deforestation is helping to reduce atmospheric CO_2 by vegetation uptake. Increasing trends in CO_2 fossil fuel fluxes indicate increasing atmospheric CO_2 levels over almost all the regions. As CO_2 gas plays a crucial role in climate change, focused mitigation efforts are required to curb CO_2 emissions from fossil fuel, particularly at hot spots regions (from LPSs) along with efforts towards increasing the vegetation cover.

4 Conclusions

Analysis of 10 years (2000–2009) of CT-2010 CO_2 fluxes gives insight into the regional variation of CO_2 fluxes over the Indian land mass. The spatial distribution of CO_2 fluxes averaged for the period 2000–2009 indicate hot spots and sink regions. CO_2 emission hot spots overlap with locations of densely clustered thermal power plants, coal mines and other industrial and urban centres. The CT-2010 fluxes clearly detect high CO_2 amount over the locations of thermal power plants having large installed capacity. CO_2 sink regions coincide with locations of dense forests with fewer industrial centres. CO_2 fossil fuel emissions show good agreement with two bottom-up inventories: the Regional Emission inventory in ASia (REAS v1.11) (2000–2009) and the Emission Database for Global Atmospheric Research (EDGAR v4.2) (2000–2009). Estimated fossil fuel emissions over the hot spot regions is ~ 500–$950\,\mathrm{gC\,m}^{-2}\,\mathrm{yr}^{-1}$ as obtained from CT-2010, EDGAR v4.2 and REAS v1.11 emission inventories. Statistically significant increasing trends are observed over the hot spot regions while negative (decreasing) trends are observed over the sink regions. The spatial distribution of fire fluxes shows higher CO_2 fluxes in the regions where fire events are frequent (dense forest cover, coal mines and oil refineries). The distribution of active fire spots shows a large number of active fire events in these regions. This demonstrates that CT-2010 fluxes can be used to identify the large emission hot spots (hardest hit regions) in India in order to mitigate the causes of pollution.

Estimated trends in CT-2010 CO_2 fluxes over the Delhi corridor regions are $3.25 \pm 1.8\,\%\,\mathrm{yr}^{-1}$ $(30 \pm 1.7\,\mathrm{TgC\,yr}^{-1})$, for Mumbai–Gujarat they are $6.21 \pm 2.77\,\%\,\mathrm{yr}^{-1}$ $(34 \pm 5.7\,\mathrm{TgC\,yr}^{-1})$, for North India they are $6.7 \pm 0.54\,\%\,\mathrm{yr}^{-1}$ $(97 \pm 12\,\mathrm{TgC\,yr}^{-1})$ and for Central India they are $\sim 1.39 \pm 1.01\,\%\,\mathrm{yr}^{-1}$ $(19.8 \pm 1.9\,\mathrm{TgC\,yr}^{-1})$. Sink regions show negative (decreasing) trends in Madhya Pradesh of $-3.2 \pm 2.48\,\%\,\mathrm{yr}^{-1}$ $(-2 \pm 0.1\,\mathrm{TgC\,yr}^{-1})$, in the Odisha–Chhattisgarh region of $-5.7 \pm 2.89\,\%\,\mathrm{yr}^{-1}$ $(-2.3 \pm 2\,\mathrm{TgC\,yr}^{-1})$, in Karnataka-Andhra Pradesh of $-1.85 \pm 2.3\,\%\,\mathrm{yr}^{-1}$ $(-1.9 \pm 3\,\mathrm{TgC\,yr}^{-1})$ and in Northeast

India of $-0.95 \pm 1.51\,\%\,\mathrm{yr}^{-1}$ $(-1 \pm 2\,\mathrm{TgC\,yr}^{-1})$. Estimated trends over the Odisha–Chhattisgarh region, Karnataka-Andhra Pradesh and Northeast India are not statistically significant since error exceeds the magnitude of the trend.

Fossil fuel fluxes show increasing trends over all the regions (A–H). Estimated trends in CT-2010 CO_2 emissions from fossil fuel burning vary between $4.37 \pm 0.28\,\%\,\mathrm{yr}^{-1}$ $(23 \pm 1.5\,\mathrm{TgC\,yr}^{-1})$ and $5.5 \pm 0.51\,\%\,\mathrm{yr}^{-1}$ $(7.2 \pm 1\,\mathrm{TgC\,yr}^{-1})$, while trends computed from REAS emissions are between $\sim 3.19 \pm 0.17\,\%\,\mathrm{yr}^{-1}$ $(0.8 \pm 0.69\,\mathrm{TgC\,yr}^{-1})$ and $3.92 \pm 0.18\,\%\,\mathrm{yr}^{-1}$ $(4.2 \pm 2.6\,\mathrm{TgC\,yr}^{-1})$ and from EDGAR v4.2 they are between $3.0 \pm 0.42\,\%\,\mathrm{yr}^{-1}$ $(4.4 \pm 2.2\,\mathrm{TgC\,yr}^{-1})$ and $4.57 \pm 0.48\,\%\,\mathrm{yr}^{-1}$ $(79.3 \pm 4.2\,\mathrm{TgC\,yr}^{-1})$. These differences may be partially due to the difference in time period of the data sets (EDGAR v4.2 data is for the period 2000–2009 while the REAS v1.11 time series is obtained from combining historical (2000–2003) and predicted (2004–2009) emissions) and partially because of differences in species and emission sources. REAS v1.11 emissions are from fossil and biofuel combustion and industrial sources while EDGAR v4.2 emissions are from fossil fuel excluding short-cycle organic carbon from biomass burning.

Although the amount of fossil fuel fluxes emitted over sinks regions are less than over hot spot regions, their emissions rates are increasing over the period. This indicates that CO_2 emission due to anthropogenic activities is increasing. CT-2010 terrestrial ecosystem fluxes show decreasing trends over most of the regions. This implies that forest cover is increasing, which is consistent with the India State of Forest Report (2009). Trends in CT-2010 total fluxes (fossil fuel, terrestrial ecosystem fluxes, fire) over the Indian region (source + sinks) show an increasing trend of $\sim 4.72 \pm 2.25\,\%\,\mathrm{yr}^{-1}$ $(25.6\,\mathrm{TgC\,yr}^{-1})$. This implies that increasing fossil fuel fluxes are more than the net terrestrial ecosystem uptake. Estimated CO_2 trends from CT-2010 fluxes over India are slightly higher than the global CO_2 growth rate $\sim 3.1\,\%\,\mathrm{yr}^{-1}$ during the period 2000–2010 (Carbon Budget, 2010).

Thus our analysis indicates that effort towards conservation and reversal of deforestation is helping to reduce atmospheric CO_2 by terrestrial ecosystem uptake over the Indian region. However increasing trends in CO_2 fossil fuel fluxes are stronger over almost all the regions. Thus focused mitigation efforts are required to curb CO_2 emission from fossil fuels particularly at hot spot regions (from LPSs) along with efforts towards increasing the vegetation cover.

data on CO$_2$ emissions, and the World Data Centre for Greenhouse Gases for providing CO$_2$ concentrations at Cape Rama, India. The authors are grateful to the Director of IITM for his constant encouragement throughout this study.

The topical editor, V. Kotroni, thanks two anonymous referees for help in evaluating this paper.

References

Behera, K., Farooquie, J. A., and Dash, A. P.: Productivity change of coal-fired thermal power plants in India: a Malmquist index approach, IMA, Journal of Management Mathematics, 22, 387–400, 2011.

Bhattcharya, S. K., Borole, D. V., Francey, R. J., Allison C. E., Steele, L. P., Krummel, P., Langenfelds, R., Masarie, K. A., Tiwari, Y. K., and Patra, P. K.: Trace gases and CO$_2$ isotope records from Cabo de Rama, India, Current Science, 97, 1336–1344, 2009.

Boden, T. A., Marland, G., and Andres, R. J.: Global, Regional, and National Fossil-Fuel CO$_2$ Emissions, Carbon Dioxide Inf. Anal. Cent., Oak Ridge Natl. Lab., US Dep. of Energy, Oak Ridge, Tenn., doi:10.3334/CDIAC/00001_V2011, 2011.

Bousquet, P., Peylin, P., Ciais, P., Le Quéré, C., Friedlingstein, P., and Tans P. P.: Regional Changes in Carbon Dioxide Fluxes of Land and Oceans Since 1980, Science, 17, 1342–1346, doi:10.1126/science.290.5495.1342, 2000.

Carbon Budget: Global Carbon Project (GCP) Report No. 7 GCP, Ten Years of Advancing Knowledge on the Global Carbon Cycle and its Management, available at: http://www.globalcarbonproject.org/products/reports.htm#otherReports, 2010.

Cherchi, A., Alessandri, A., Masina, S., and Navarra, A.: Effects of increased CO$_2$ levels on monsoons, Clim. Dynam. 37, 83–101, doi:10.1007/s00382-010-0801-7, 2011.

Dalvi, M., Beig, G., Patil, U., Kaginalkar, A., Sharma, C., and Mitra, A. P.: A GIS based methodology for gridding large scale emission inventories: Application to carbon-monoxide emissions over Indian region, Atmos. Environ., 40, 2995–3007, doi:10.1016/j.atmosenv.2006.01.013, 2006.

DoE and EPA: Department of Energy and Environmental Protection Agency: Carbon Dioxide Emissions from the Generation of Electric Power in the United States, Washington, DC 20585(DoE) and 20460(EPA), 19 pp., 2000.

EPA: Environmental Protection Agency, Carbon Dioxide as a Fire Suppressant: Examining the Risks, EPA430-R-00-002, 2000.

Fadnavis, S. and Beig, G.: Seasonal variation of trend in temperature and ozone over the tropical stratosphere in the Northern Hemisphere, J. Atmos. Sol.-Terr. Phy., 68, 1952–1961, 2006.

Garg, A., Bhattacharya, S., Shukla, P. R., and Dadhwal, V. K.: Regional and sectoral assessment of greenhouse gases emissions in India, Atmos. Environ., 35, 2679–2695, 2001.

Garg, A., Kapshe, M., Shukla, P. R., and Ghodh, D.: Large point source (LPS) emission from India: Regional and sectoral analysis, Atmos. Environ., 36, 213–224, doi:10.1016/S1352-2310(01)00439-3, 2002.

Garg, A., Shukla, P. R., and Kapshe, M.: The sectoral trends of multigas emissions inventory of India, Atmos. Environ., 40, 4608–4620, 2006.

Ghude, S. D., Fadnavis, S., Beig, G., Polade, S. D., and van der, A. R. J.: Detection of surface emission hot spots, trends, and seasonal cycle from satellite-retrieved NO$_2$ over India, J. Geophys. Res., 113, D20305, doi:10.1029/2007JD009615, 2008.

Giglio, L., van der Werf, G. R., Randerson, J. T., Collatz, G. J., and Kasibhatla, P.: Global estimation of burned area using MODIS active fire observations, Atmos. Chem. Phys., 6, 957–974, doi:10.5194/acp-6-957-2006, 2006.

Gurney, K. R., Law, R. M., Denning, A. S., Rayner, P. J., Baker, D., Bousquet, P., Bruhwiler, L., Chen, Y.-H., Ciais, P., Fan, S., et al.: Towards robust regional estimates of CO$_2$ sources and sinks using atmospheric transport models, Nature, 415, 626–630, doi:10.1038/415626a, 2002.

Guttikunda, S. K and Jawar, P.: Atmospheric emissions and pollution from the coal-fired thermal power plants in India, Atmos. Environ., 92, 449–460, doi:10.1016/j.atmosenv.2014.04.057, 2014.

Hungershoefer, K., Breon, F.-M., Peylin, P., Chevallier, F., Rayner, P., Klonecki, A., Houweling, S., and Marshall, J.: Evaluation of various observing systems for the global monitoring of CO$_2$ surface fluxes, Atmos. Chem. Phys., 10, 10503–10520, doi:10.5194/acp-10-10503-2010, 2010.

IEA: International Energy Agency, CO$_2$ emission from fuel combustion highlights, 2011.

INCCA: Indian Network for Climate Change Assessment, India: Greenhouse Gas Emissions (2007), Ministry of Environment and Forests Government of India, 2010.

India State of Forest Report: Forest Survey of India, Ministry of Environment & Forests, Govt. of India, Dehradun, 1–12, 2009.

IPCC, 2007: Forster, P., Ramaswamy, V., Artaxo, P., Berntsen, T., Betts, R., Fahey, D. W., Haywood, J., Lean, J., Lowe, D. C., Myhre, G., Nganga, J., Prinn, R., Raga, G., Schulz, M., and Van, D. R., Changes in Atmospheric Constituents and in Radiative Forcing, in: Climate Change 2007: The Physical Science Basis. Contribution of Working Group I to the Fourth Assessment Report of the Intergovernmental Panel on Climate Change, edited by: Solomon, S., Qin, D., Manning, M., Chen, Z., Marquis, M., Averyt, K. B., Tignor, M., Miller, H. L., Cambridge University Press, Cambridge, United Kingdom and New York, NY, USA, 2007.

Jacobson, A. R., Gruber, N., Sarmiento, J. L., Gloor, M., and Mikaloff, Fletcher, S. M.: A joint atmosphere-ocean inversion for surface fluxes of carbon dioxide: I. Methods and global-scale fluxes, Global Biogeochem. Cy., 21, GB1019, 1–13, doi:10.1029/2005GB002556, 2007.

Jiang, X., Chahine, M. T., Olsen, E. T., Chen, L. L., and Yung, Y. L.: Inter-annual variability of mid-tropospheric CO$_2$ from Atmospheric Infrared Sounder, Geophys. Res. Lett., 37, L13801, doi:10.1029/2010GL042823, 2010.

JRC/PBL: EDGAR version 4.2 FT2010, Joint Research Centre/PBL Netherlands Environmental Assessment Agency, Emission Database for Global Atmospheric Research (EDGAR), available at: http://edgar.jrc.ec.europa.eu (last access: 5 June 2015), 2012.

Latha, R. and Murthy, B. S.: Natural reduction of CO$_2$ observed in the pre-monsoon period at the coastal station Goa, Meteorol. Atmos. Phys., 115, 73–80, 2012.

Mandal, B., Majumder, B., Bandyopadhyay, P. K., Hazra, G. C., Gangopadhyay, A., Samantaray, R. N., Mishra, A. K., Chaud-

hury, J., Saha, M. N., and Kundu, S., 2006. The potential of cropping systems and soil amendments for carbon sequestration in soils under long term experiments in subtropical India, Glob. Change Biol., 13, 357–369, 2006.

May, W.: The sensitivity of the Indian summer monsoon to a global warming of 2 °C with respect to pre-industrial times, Clim. Dynam., 37, 1843–1868, DOI 10.1007/s00382-010-0942-8, 2011.

Meehl, G. A. and Washington, W. M.: South Asian summer monsoon variability in a model with a doubled atmospheric carbon dioxide concentration, Science, 260, 1101–1104, 1993.

Meehl, G. A., Washington, W. M., Arblaster, J. M., Bettge, T. W., and Strand Jr., W. G.: Anthropogenic Forcing and Decadal Climate Variability in Sensitivity Experiments of Twentieth- and Twenty-First-Century Climate, J. Climate, 13, 3728–3744, 2000.

Ohara, T., Akimoto, H., Kurokawa, J., Horii, N., Yamaji, K., Yan, X., and Hayasaka, T.: An Asian emission inventory of anthropogenic emission sources for the period 1980–2020, Atmos. Chem. Phys., 7, 4419–4444, doi:10.5194/acp-7-4419-2007, 2007.

Olivier, J. G. J. and J. J. M. Berdowski: Global emissions sources and sinks, in: The Climate System, edited by: Berdowski, J., Guicherit, R., and Heij, B. J., 33–78, A. A. Balkema Publishers/Swets & Zeitlinger Publishers, Lisse, the Netherlands, ISBN: 90 5809 255 0, 2001.

Olivier, J. G. J., Berdowski, J. J. M., Peters, J. A. H. W., Bakker, J., Visschedijk en, A. J. H., and Bloos, J.-P. J.: Applications of EDGAR. Including a description of EDGAR 3.0: reference database with trend data for 1970–1995, RIVM, Bilthoven, RIVM report no. 773301 001/ NOP report no. 410200 051, 2001.

Peters, W., Jacobson, A. R., Sweeney, C., A. E., Conway, T. J., Masarie, K., Miller, J. B., Bruhwiler, Lori, M. P., Pétron, G., Hirsch, A. I., Worthy, D. E. J., van der Werf, G. R., Randerson, J. T., Wennberg, P. O., Krol, M. C., and Tans, P. P.: An atmospheric perspective on North American carbon dioxide exchange: Carbon Tracker, PNAS, 104, 18925–18930, 2007.

Randel, W. J. and Cobb, J. B.: Coherent variations of monthly mean total ozone and lower stratospheric temperature, J. Geophys. Res., 99, 5433–5477, 1994.

Rayner, P., Enting, J. I. G., Francey, R. J., and Langenfelds, R. L.: Reconstructing the recent carbon cycle from atmospheric CO_2, d13C and O_2/N_2 observations, Tellus-B, 51, 213–232, 1999.

Rivier, L., Peylin, P., Ciais, P., Gloor, M., Rödenbeck, C., Geels, C. Karstens, U., Bousquet, P., Brandt, J., Heimann, M., and Aerocarb experimentalists: European CO_2 fluxes from atmospheric inversions using regional and global transport models, Climatic Change, doi:10.1007/s10584-010-9908-4, 2010.

Rödenbeck, C., Houweling, S., Gloor, M., and Heimann, M.: CO_2 flux history 1982–2001 inferred from atmospheric data using a global inversion of atmospheric transport, Atmos. Chem. Phys., 3, 1919–1964, doi:10.5194/acp-3-1919-2003, 2003.

Schuck, T. J., Brenninkmeijer, C. A. M., Baker, A. K., Slemr, F., von Velthoven, P. F. J., and Zahn, A.: Greenhouse gas relationships in the Indian summer monsoon plume measured by the CARIBIC passenger aircraft, Atmos. Chem. Phys., 10, 3965–3984, doi:10.5194/acp-10-3965-2010, 2010.

Shindell, D. and Faluvegi, G.: The net climate impact of coal-fired power plant emissions, Atmos. Chem. Phys., 10, 3247–3260, doi:10.5194/acp-10-3247-2010, 2010.

Tans, P. P., Fung, I. Y, and Takahashi, T.: Observational constraints on the global atmospheric CO_2 budget, Science, 247, 1431–1439, doi:10.1126/science.247.4949.1431, 1990.

Tiwari, Y. K., Patra, P. K., Chevallier, F., Francey, R. J., Krummel, P. B., Allison, C. E., Revadekar, J. V., Chakraborty, S., Langenfeld, R. L., Bhattacharya, S. K., Borole, D. V., Ravi Kumar, K., and Steele, L. P.: Carbon dioxide observations at Cape Rama, India for the period 1993–2002: implications for constraining Indian emission, Current Science, 101, 1562–1568, 2011.

van der Werf, G. R., Randerson, J. T., Giglio, L., Collatz, G. J., Kasibhatla, P. S., and Arellano Jr., A. F.: Interannual variability in global biomass burning emissions from 1997 to 2004, Atmos. Chem. Phys., 6, 3423–3441, doi:10.5194/acp-6-3423-2006, 2006.

User Guide for CO_2 Baseline Database for the Indian Power Sector, Version 6.0: Government of India Ministry of Power Central Electricity Authority, Sewa Bhawan, R. K. Puram, New Delhi-66, 2011.

Wang, J., Jiang, X., Chahine, M., Liang, M., Olsen, M. ,Chen, L., Licata, S., Pagano, T., and Yung, Y. L.: The influence of tropospheric biennial oscillation on mid tropospheric CO_2, Geophys. Res. Lett., 38, L20805, doi:10.1029/2011GL049288, 2011.

Wang, R., Tao, S., Wang, W., Liu, J., Shen, H., Shen, G., Wang, B., Liu, X., Li, W., Huang, Y., Zhang, Y., Lu, Y., Chen, H., Chen, Y., Wang, C., Zhu, D., Wang, X., Li, B., Liu, W., and Ma, J.: Black carbon emissions in China from 1949 to 2050, Environ. Sci. Technol., 46, 7595–7603, 2012.